Geology of three dioritic plutons in Velfjord, Nordland

CALVIN G. BARNES, TORE PRESTVIK, ØYSTEIN NORDGULEN & MELANIE A. BARNES

Barnes,C.G., Prestvik,T., Nordgulen,Ø. & Barnes, M.A. 1992: Geology of three dioritic plutons in Velfjord, Nordland. *Nor. geol. unders. Bull. 423,* 41-54.

Dioritic plutons in the Velfjord area of Nordland intrude calc-silicates and migmatitic pelites of the Helgeland Nappe Complex (HNC). The three largest plutons were emplaced in a zone of NNW-SSE regional strike rather than the more typical NE-SW strike. The plutons postdate Caledonian F_2 structures; however, anatectic granites increase in abundance toward the plutons, which suggests emplacement and subsequent partial melting of the pelitic host rocks soon after peak metamorphism. The dioritic and granitic bodies were deformed with interstitial melt present; deformation continued during cooling to greenschist facies conditions. Structural position, style and timing of deformation, and asymmetric zoning of the plutons are consistent with intrusion into a dilatant part of a regional sinistral shear zone.

The northernmost, alkali-calcic (Hillstadfjellet) pluton consists of an older dioritic unit with widely variable major element contents and a younger unit that is asymmetrically zoned from monzodiorite, through monzonite, to quartz monzonite. These younger rocks display at least two compositional trends, one richer in K_2O, that are probably not related by simple fractional crystallization. The central, dioritic, alkali-calcic (Akset-Drevli) pluton is distinguished by prominent flow foliation (locally strongly deformed), cm-scale plagioclase phenocrysts, and abundant oxides and apatite. It has lower $Mg/(Mg+Fe_T)$, generally higher TiO_2, and slightly higher normalized Ce/Yb than the other plutons. The southern, calc-alkalic (Sausfjellet) pluton is zoned, E to W, from pyroxene diorite to pyroxene-biotite-hornblende-quartz monzodiorite. It has higher $Mg/(Mg+Fe_T)$ and lower TiO_2 than the Akset-Drevli pluton, and normalized Ce/Yb ranges from 3 to 18. The plutons are distinct from the peraluminous anatectic granites, whose Al_2O_3, Na_2O, and REE abundances suggest an origin by in situ partial melting of pelitic host rocks. Geochemical differences between the Velfjord plutons suggest that parental magma compositions varied from one pluton to the next, that at least two of the plutons had more than one parental magma, and that each magma followed a distinct differentiation trend.

Calvin G. Barnes & Melanie A. Barnes, Department of Geosciences, Texas Tech University, Lubbock, Texas 79409, USA
Tore Prestvik, Department of Geology & Mineral Resources Engineering, Norwegian Institute of Technology, N-7034 Trondheim, Norway
Øystein Nordgulen, Geological Survey of Norway, P.O.Box 3006, N-7002 Trondheim, Norway

Introduction

The Bindal Batholith represents one of the largest occurrences of granitic magmatism in the Norwegian Caledonides (Stephens et al. 1985). Most plutons in the batholith are tonalitic to granitic in composition; however, sparse gabbroic to dioritic bodies are widespread (e.g., Tørudbakken & Mickelson 1986). Examples of dioritic magmatism in the province are provided by plutons of the Velfjord massifs (Kollung 1967), which occupy a central position in the batholith (Fig. 1). These plutons range from olivine gabbro to biotite-quartz monzonite, but are predominantly dioritic to monzodioritic in composition. Although the relatively mafic Velfjord plutons are in close proximity to granitic rocks of the batholith, the temporal and petrologic relations between them are not well known. For this reason, we have undertaken a detailed study of the petrogenesis of the three largest plutons in the area, which are herein informally referred to as the Velfjord plutons, and their possible relations to the batholith as a whole.

In this contribution, we report on the field relations, zoning patterns, and petrographic characteristics of the Velfjord plutons along with a reconnaissance geochemical study. The data suggest that each of the plutons is internally complex, and that each is petrogenetically distinct from the others and from granitic rocks of the Bindal Batholith.

Geologic setting

The plutons are intrusive into metasedimentary rocks of the Helgeland Nappe Complex (HNC) of the Uppermost Allocthon (Stephens et al. 1985). They occupy a part of the HNC where the regional strike is NNW-SSE. This is distinct from the Bindal area to the south and the area north of Vefsnfjord (north of Velfjord), where a NE-SW strike is more typical. A subhorizontal lineation is common in granitic and metamorphic rocks in the zones with NE-SW strike but is less pronounced in the zone with NNW-SSE strike.

In the Velfjord area, HNC rocks comprise three thrust sheets separated by east- to northeast-dipping faults (Thorsnes & Løseth 1991). The lowest sheet is host to the plutons and consists of variably migmatitic quartzofeldspathic schist and gneiss, calc-silicate schist, and marble. These rocks are within the sillimanite zone (Myrland 1972). The middle sheet consists of basal mafic and ultramafic rocks unconformably overlain by metamorphosed clastic and calc-silicate rocks. The upper sheet is lithologically similar to the lower one (Thorsnes & Løseth 1991).

Myrland (1972) and Kollung (1967) interpreted the plutons to postdate D_2 deformation because D_2 structures in the wall rocks are deflected by the plutons and because the wall rocks display a pronounced increase in metamorphic grade near the intrusions (see below; Myrland 1972). Moreover, Thorsnes & Løseth (1991) suggested that thrusting within the HNC was related to D_2 and that thrusting occurred before intrusion of the Velfjord plutons (also see Bucher-Nurminen 1988). This conclusion is supported by intrusive relations of a small dioritic body immediately to the east of the Sausfjellet pluton (the Markafjellet pluton of Kollung 1967) that cuts faults between the lower, middle, and upper thrust sheets (Thorsnes & Løseth 1991). If this pluton belongs to the same magmatic event as the Velfjord plutons, then Velfjord magmatism occurred after thrusting.

Kollung (1967) interpreted the Velfjord massif to be older than granitic rocks of the Bindal Batholith because the Velfjord rocks are intruded by granitic dikes. However, many of the granitic rocks that intrude the Velfjord plutons are compositionally distinct from, and may not be related to the nearby Bindal granites (see below). Thus, we suspect that there are no unequivocal cross-cutting relations between the Velfjord plutons and granitic rocks of the Bindal Batholith. Such problems emphasize the need for precise radiometric dating of the units (in progress).

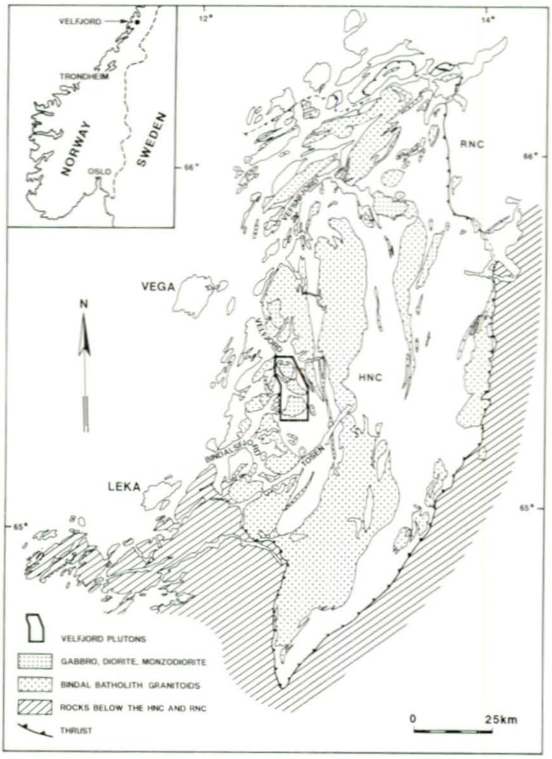

Fig. 1. Regional geologic setting, showing the location of the Velfjord plutons within the Bindal Batholith. The gabbroic to granitic plutons of the batholith intrude metasedimentary rocks (no ornament) of the Uppermost Allochthon, which in this region comprises the Helgeland Nappe Complex (HNC) and the Rødingsfjellet Nappe Complex (RNC).

The Velfjord plutons

General Contact Relations

The plutons of the Velfjord area have not been formally named; therefore, for ease of discussion, the large plutons are referred to informally, from north to south, as the Hillstadfjellet pluton, the Akset-Drevli pluton, and the Sausfjellet pluton. A small monzonitic body that crops out near Aunet, east of Hommelstø (Fig. 2), is called the Aunet monzonite.

The contacts between the plutons and their wall rocks generally display steep to moderate dips. An exception to this is apparent along the northern contact of the Akset-Drevli pluton, where sill-like apophyses of the pluton intrude wall rocks in the Hommelstø area. Contacts with marble and calc-silicate schists are generally rather sharp, although in many localities contacts are marked by a series of dioritic dikes that become more abundant as the pluton is approached. In some localities the grain size of the plutonic rocks decreases near contacts.

Contacts with migmatitic pelitic rocks are generally marked by zones of heterogeneous, equigranular to porphyritic, garnet- and sillimanite-bearing granite (Figs. 2 and 3). These zones range from a few meters to as much as 300 m wide, e.g., along the southern contact of the Akset-Drevli pluton (Fig. 2). In general, these granitic bodies are gradational outward into diatectic rocks and then into migmatitic gneiss. Where intrusive relations were observed, the contact granites are intrusive into the Velfjord plutons. Near Lisjøen, along the eastern border of the Hillstadfjellet pluton, the granites are separated from quartz monzonitic rocks of the pluton by a zone of garnet-bearing quartz diorite.

Contact relations between the Hillstadfjellet, Akset-Drevli, and Aunet bodies were observed in the area east of Hommelstø. Dioritic rocks of the Akset-Drevli pluton and of the first intrusive stage of the Hillstadfjellet pluton are intruded by porphyritic diorite of the second stage of the Hillstadfjellet pluton. Dikes of the Aunet monzonite cut all three units. Cross-cutting relations between the first stage of the Hillstadfjellet pluton and the Akset-Drevli pluton were not observed. The relative timing of intrusion of the Sausfjellet pluton is unknown.

All three plutons and some contact granites are cut by medium- to fine-grained felsic dikes that range in composition from tonalitic to granitic. They average about one meter in width and typically carry biotite or biotite + muscovite. Mafic dikes (microgabbro to coarse-grained gabbro and diorite) were observed in all three plutons.

Deformation

All of the Velfjord plutons show evidence of deformation. The degree of deformation grades from minor bending of plagioclase, through development of subgrains in quartz and plagioclase, to grain-size reduction and recrystallization along grain boundaries and, locally, to development of protomylonitic fabrics with porphyroclastic textures and rare ribbon quartz. Deformation is typically more pronounced in the outer parts of the plutons. Most late felsic dikes are undeformed or weakly deformed, but some display stronger deformation than their host dioritic rocks.

A wide range of minerals were stable during deformation. In some instances, deformation occurred in the stability field of plagioclase, clinopyroxene (cpx), and orthopyroxene (opx); with undeformed or weakly deformed late-magmatic biotite and amphibole. In other cases, biotite and actinolitic amphibole (after pyroxene) were the stable mafic phases. Deformation also encompassed the lower-temperature assemblage biotite, epidote, sodic plagioclase, and quartz. This petrographic evidence indicates that deformation began when the plutons contained a melt phase and continued during cooling to greenschist-facies conditions.

The granitic rocks at the margins of the plutons record a similar history of deformation. Their tectonic fabrics are typically better developed than those in the adjacent plutons.

Zoning and Internal Structures

Hillstadfjellet pluton

The rocks of this pluton are generally massive or weakly foliated. The pluton contains several large metasedimentary screens (Fig. 2), metasedimentary xenoliths that range from cm to several tens of meters in size, and rare peridotitic xenoliths. The first intrusive stage is represented by a gabbroic to dioritic body exposed in the northeastern part of the pluton (Fig. 2). The second stage ranges in composition from monzodiorite (with rare diorite) to quartz monzonite. This unit is asymmetrically zoned, with the most mafic rocks in the western and southern parts of the intrusion, quartz-rich rocks in the east (between the large metasedimentary screens and rocks of the first stage), and monzonitic rocks in the north and between the mafic rocks and the quartz-rich ones (Fig. 2). Relative intrusive relationships are demonstrated by the inclusion of angular xenoliths of first-stage rocks in the second stage.

The primary mafic minerals in the first-stage rocks were cpx, opx, and hornblende. In the

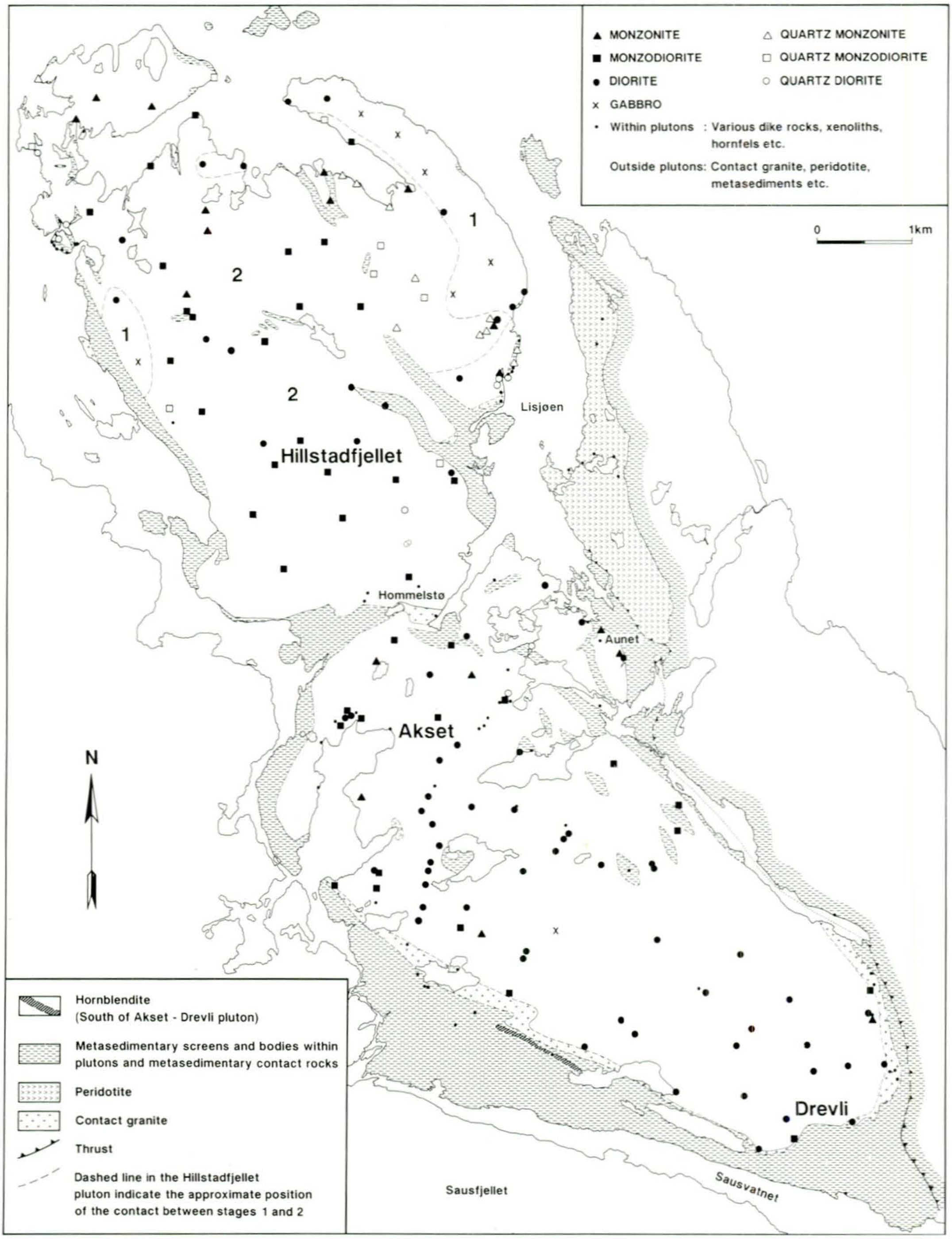

Fig. 2. Geology of the Hillstadfjellet and Akset-Drevli plutons. The numbers 1 and 2 indicate the locations of stages 1 and 2 of the Hillstadfjellet pluton.

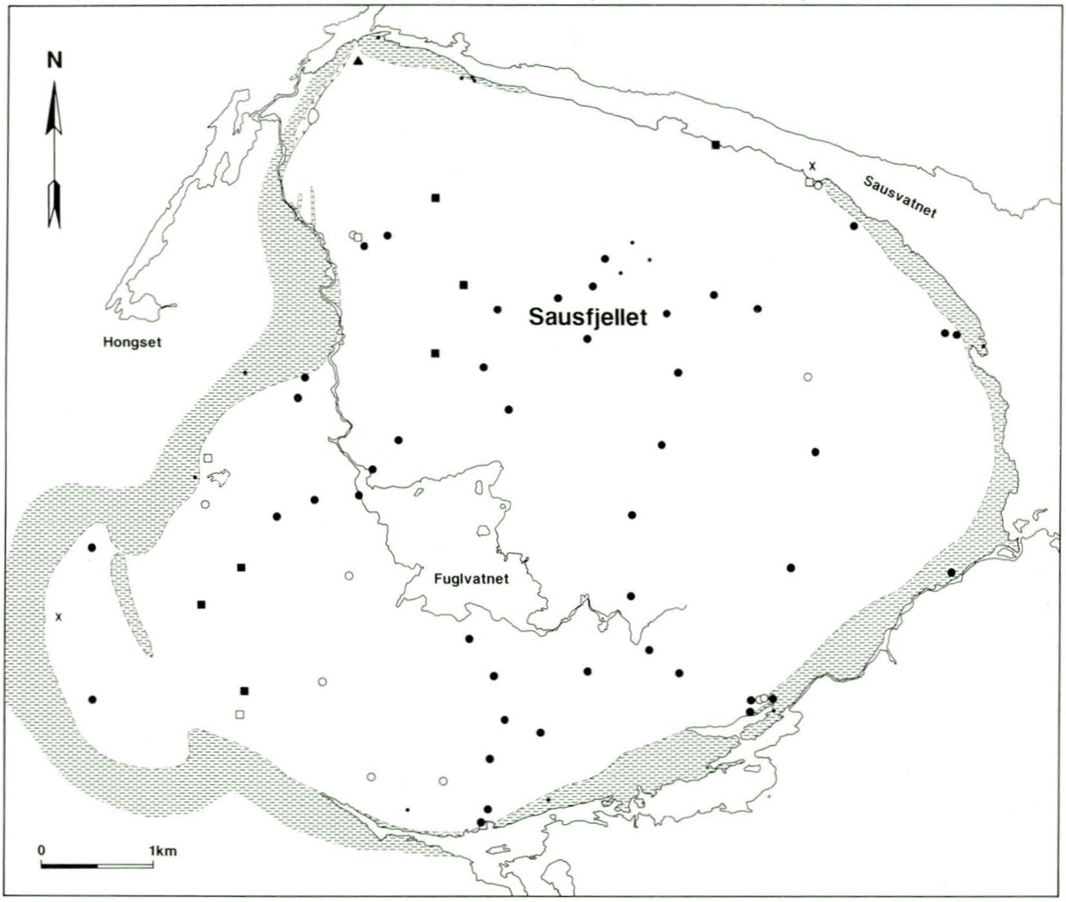

Fig. 3. Geology of the Sausfjellet pluton. Symbols as in Fig. 2.

second stage, primary cpx, opx, and biotite in the mafic western rocks give way to the east to cpx + opx + biotite + hornblende, then biotite + hornblende, then biotite. These relations have been obscured by recrystallization at lower temperatures, particularly in zones of high strain (compare Figs. 4a and 4b).

Akset-Drevli pluton

This pluton is predominantly dioritic, but contains minor monzodiorite and monzonite, especially in its northern parts. The typical primary mafic assemblage is cpx, opx, and biotite (±amphibole); however, olivine is present locally, especially in samples from the southeastern part of the pluton (Fig. 4c).

The Akset-Drevli pluton is characterized by abundant, large plagioclase phenocrysts (2 to 3 cm in maximum dimension) that commonly define a well-developed foliation. This foliation was originally magmatic, but has been warped and folded in zones of high strain (Fig. 4d). Some samples display high-temperature deformation in which plagioclase crystals have been bent by up to 60°.

Metasedimentary screens and xenoliths are locally abundant in the pluton, and some of the calc-silicate xenoliths contain Cr-rich grossular garnet (Prestvik, 1974). Two peridotite xenoliths ($<$ 250 m) crop out in the western part of the body.

Sausfjellet pluton

This pluton is predominantly dioritic, but contains sparse quartz diorite and quartz monzodiorite in its southwestern part (Fig. 3). A

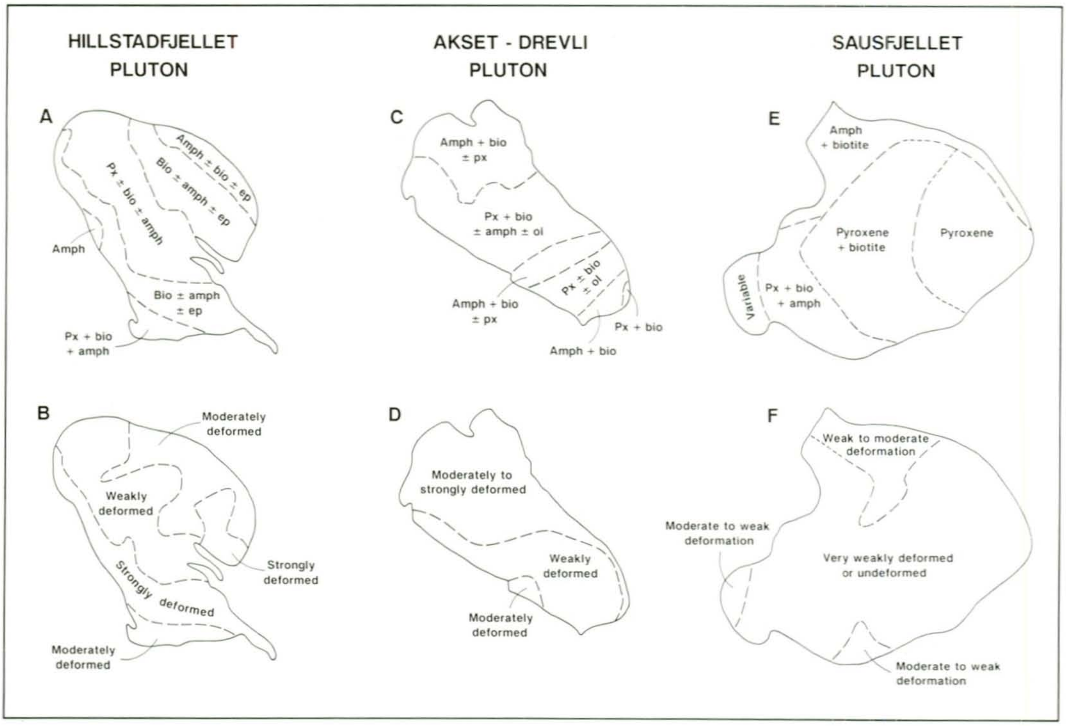

Fig. 4. A. Distribution of mafic minerals in the Hillstadfjellet pluton. B. Deformation patterns in the Hillstadfjellet pluton. C. Distribution of mafic minerals in the Akset-Drevli pluton. D. Deformation patterns in the Akset-Drevli pluton. E. Distribution of mafic minerals in the Sausfjellet pluton. F. Deformation patterns in the Sausfjellet pluton.

pronounced asymmetric zonation is displayed by the primary mafic assemblages (Fig. 4e), which range from cpx and opx in the east, through a central zone of cpx, opx, and biotite, to cpx, opx, biotite, and amphibole in the southwest. Samples collected near contacts are generally the only ones to show appreciable deformation (Fig. 4f) and they commonly contain the subsolidus mafic assemblage of amphibole and biotite.

Magmatic foliation is common in Sausfjellet samples, as is schlieren banding. On Sausfjellet, blocks of schlieren-banded diorite >100 m across are surrounded by weakly banded to massive diorite. The presence of the blocks suggests an early history during which the banding formed along the pluton's margins by flow segregation, followed by stoping of the blocks during the final stages of intrusion.

Petrography

Petrographic descriptions are based on inspection of over 450 thin-sections. Where cited, plagioclase, alkali feldspar, and amphibole compositions were determined by electron microprobe analysis (C. Barnes and T. Prestvik, unpubl. data).

First-stage gabbro and diorite of the Hillstadfjellet pluton display relict hypidiomorphic granular texture that is now partly to completely recrystallized by granulation and local mylonitization. Primary cpx, opx, poikilitic brown calcic amphibole, and reddish-brown biotite are variably altered to actinolitic amphibole and chlorite. Epidote has partly replaced plagioclase. Apatite, ilmenite, magnetite, and chalcopyrite are accessory minerals.

Second-stage rocks have variably deformed hypidiomorphic granular texture. From southwest to northeast, the rocks become more porphyritic (plagioclase) and the grain size of the groundmass decreases slightly. Plagioclase (An_{50}-An_{16}) is normally zoned and is typically resorbed and rimmed by microcline. Quartz, where present, is interstitial. In the least deformed monzodioritic samples, pyroxenes are rimmed by olive-green edenitic amphibole. In monzonitic rocks only relict pyroxene is present and olive-green edenitic amphibole is rimmed by a blue-green ferro-edenite. Accessory minerals are apatite, allanite, zircon, ilmenite, magnetite, chalcopyrite, pyrite, sphene, and tourmaline.

The large plagioclase phenocrysts (An_{56}-An_{30}) in the Akset-Drevli pluton not only define the fabric but control the textural relations. Some cpx and opx grains are euhedral and, along with anhedral, pyroxene-rimmed olivine, are best described as intergranular. The pyroxenes are also present as interstitial minerals along with reddish-brown biotite, relatively abundant oxides, and mm-scale prismatic apatite. Primary pargasitic amphibole is rare in this pluton; it occurs as rims on pyroxenes. Microcline is present interstitially and in resorption channels in plagioclase; quartz is interstitial. Along with the aforementioned apatite, accessory minerals are ilmenite, magnetite, and rare zircon, allanite, and pyrite.

The texture of rocks from the Sausfjellet pluton ranges from subophitic to hypidiomorphic granular. Plagioclase is generally normally zoned from An_{58} to An_{36}. Intergranular to interstitial pyroxenes are partly replaced by reddish-brown biotite and olive-green hornblende. Quartz and microcline are interstitial. Accessory apatite is present in granular, prismatic, and acicular habits. Zircon, allanite, ilmenite, magnetite, anhedral to poikilitic sphene, and epidote are the other accessory phases. Subsolidus alteration of pyroxene has resulted in growth of actinolitic and cummingtonitic amphibole, quartz, and rare greenish biotite.

The Aunet monzonite contains abundant tabular phenocrysts of perthitic alkali feldspar ($\approx Or_{66}Ab_{31}An_3$) as much as 10 cm in diameter and plagioclase phenocrysts ($\approx An_{22}$) as much as 1 cm long set in an hypidiomorphic granular groundmass. The groundmass consists of plagioclase, microcline, poikilitic to prismatic olive-green to blue-green ferro-edenite with relict pyroxene cores, and poikilitic yellow-brown biotite. Quartz, apatite, sphene, zircon, ilmenite, magnetite, chalcopyrite, and epidote are accessory phases.

The granitic rocks adjacent to the Velfjord plutons are widely variable in texture and mineralogy. They are generally hypidiomorphic granular and range from porphyritic (alkali feldspar ± plagioclase phenocrysts) to equigranular. Plagioclase (≈An35), microcline, quartz, and biotite are common to all of these rocks. Some contain accessory amphibole (ferroan pargasitic hornblende), allanite, apatite, zircon, sphene, opaque minerals, and epidote. Others contain assemblages typical of strongly peraluminous granites, with muscovite, garnet, and accessory prismatic sillimanite, opaque minerals, apatite, and zircon. One sample also contains relatively abundant opx (En36) and rare green spinel.

Granitic dikes that cut the contact granites and the plutons are hypidiomorphic granular to aplitic. Although some dikes contain calcic amphibole, biotite is the most common mafic mineral, with or without white mica. Allanite, zircon, epidote, and opaque minerals are typical accessory phases.

Geochemistry

Analytical Methods

Samples from the Bindal Batholith and some samples of the Velfjord plutons were analyzed by X-ray fluorescence (XRF) at Midland Earth Science Associates, Nottingham. For the remaining samples, major- and most trace-element analyses were done by XRF at NTH or by inductively-coupled atomic emission spectrometry at Texas Tech University. The rare-earth elements (REE), Ta, Th, Hf, and U, were analyzed by instrumental neutron activation analysis at Imperial College, London.

Results

Representative results are presented in Table 1. Samples of granitic rocks from the Bindal batholith are from localities within 5 km of the Velfjord plutons.

The Hillstadfjellet pluton is alkali-calcic, with an alkali-lime index of about 53. The first stage is distinct from the second in its lower SiO_2 and Na_2O, its widely variable TiO_2 and Al_2O_3, and its higher CaO contents (Fig. 5). The particularly wide range of Al_2O_3 , TiO_2 and Sr contents (Table 1; Fig. 5;) suggests that compositions are controlled by variable accumulation of plagioclase and pyroxene. This is supported by the slight positive Eu anomalies of Al-rich first stage samples (Fig. 7a).

Table 1. Major and trace element compositions of representative samples.*

	Hillstadfjellet pluton										Aunet monzonite		Akset-Drevli pluton							
	—First stage—		Secong stage+																	
sample	VF48	72.83	72.73	VF42	VF43	91.12	72.80	VF41	72.84	VF44	72.59	90.06	N87-27	72.40	VF53	73.103	N48 91	VF50	VF59	72.61
SiO_2	50.10	50.70	51.81	54.83	56.76	58.47	60.16	56.36	61.02	62.16	59.38	61.19	46.69	48.42	49.93	50.68	51.13	51.80	55.44	55.48
TiO_2	0.41	0.38	1.72	1.09	1.12	1.16	1.13	1.13	0.96	0.88	0.95	0.81	2.08	0.83	2.86	1.40	2.19	1.87	1.60	1.92
Al_2O_3	24.26	20.76	19.24	19.53	17.95	17.96	18.32	18.76	17.77	16.42	17.99	17.59	19.82	6.17	14.79	15.83	18.54	15.40	17.51	17.48
Fe_2O_3	4.26	6.06	8.81	6.59	6.25	6.14	4.93	6.22	5.09	5.26	5.71	4.75	10.37	9.07	12.80	10.51	9.14	11.49	7.94	9.02
MnO	0.07	0.10	0.13	0.13	0.14	0.13	0.11	0.13	0.11	0.17	0.09	0.08	0.13	0.14	0.18	0.16	0.12	0.19	0.15	0.15
MgO	2.81	5.02	3.10	2.66	2.64	1.86	1.18	2.10	1.59	1.60	1.35	1.16	4.19	17.86	4.44	7.08	3.19	5.54	2.40	2.29
CaO	12.34	9.48	7.68	7.12	5.69	4.34	2.12	6.23	3.50	3.26	4.17	3.45	10.60	16.73	6.97	7.45	8.28	8.24	5.57	4.90
Na_2O	2.95	3.87	4.39	4.91	4.86	4.41	5.19	5.40	5.29	5.07	5.12	4.76	3.56	0.63	3.92	3.04	3.76	2.72	4.68	4.32
K_2O	1.03	1.46	2.12	2.59	3.40	4.39	5.70	2.54	3.32	4.10	4.10	5.04	0.62	0.13	2.52	1.31	2.21	1.75	3.31	3.32
P_2O_5	0.14	1.31	0.73	0.30	0.42	0.47	0.39	0.47	0.42	0.44	0.36	0.23	1.17	0.05	1.41	0.67	1.22	0.27	0.70	1.01
LOI	1.58	n.d.	0.07	0.05	0.42	0.29	n.d.	0.55	n.d.	0.46	n.d.	0.37	0.17	0.88	0.16	0.14	0.14	0.48	0.69	n.d.
Total	99.95	99.14	99.80	99.80	99.65	99.62	99.23	99.89	99.07	99.82	99.22	99.43	99.40	100.91	99.98	98.27	99.92	99.75	99.99	99.89
Rb	40	72	60	74	76	145	141	79	115	137	166	197	11	2	78	23	50	64	74	81
Sr	1295	1592	950	972	716	569	447	1057	728	536	473	429	1197	79	567	707	768	333	717	633
Zr	51	26	36	200	114	457	276	179	212	271	438	404	55	27	209	156	212	199	307	28
Y	14	16	37	26	32	53	27	34	29	43	40	32	28	16	49	23	39	44	41	44
Nb	5	n.d.	11	43	41	27	n.d.	44	n.d.	57	20	21	5	11	22	11	n.d.	22	25	n.d.
Ba	214	443	974	709	953	1067	3118	861	1138	1016	723	694	299	16	606	585	851	431	1075	1495
Sc	15	2.2	15	12	13	n.d.	7.4	10	5.7	7	5	n.d.	18	n.d.	18	n.d.	n.d.	24	14	14.6
V	14	19	143	120	108	55	17	121	39	48	63	28	230	178	291	196	202	192	105	102
Cr	57	16	89	12	23	n.d.	27	22	32	3	59	n.d.	51	1493	47	236	21	84	20	36
Ni	11	5	27	8	13	2	6	4	0	3	20	5	33	245	30	81	19	22	15	3
Cu	9	11	3	13	14	10	3	8	3	7	16	31	48	21	92	94	167	23	40	28
Zn	29	63	105	68	71	88	87	76	80	91	84	50	92	44	127	87	85	103	96	110
Th	2	n.d.	n.d.	9	0	n.d.	n.d.	18	n.d.	22	28.4	40.5	5	n.d.	14	n.d.	n.d.	6	10	n.d.
La	13	37.1	n.d.	42	55	n.d.	n.d.	59	63.1	76	90.6	78.7	50	n.d.	88	n.d.	n.d.	27	64	n.d.
Ce	23	67	n.d.	101	112	n.d.	n.d.	118	116	159	146.8	119.5	107	n.d.	201	n.d.	n.d.	71	133	n.d.
Nd	15	29	n.d.	43	41	n.d.	n.d.	44	44	57	58.3	49.8	47	n.d.	82	n.d.	n.d.	38	53	n.d.
Sm	n.d.	5.34	n.d.	n.d.	n.d.	n.d.	n.d.	n.d.	7.29	n.d.	12.6	7.5	n.d.	n.d.	n.d.	n.d.	n.d.	n.d.	n.d.	n.d.
Eu	n.d.	2.28	n.d.	n.d.	n.d.	n.d.	n.d.	n.d.	2.43	n.d.	1.33	1.7	n.d.	n.d.	n.d.	n.d.	n.d.	n.d.	n.d.	n.d.
Tb	n.d.	0.5	n.d.	n.d.	n.d.	n.d.	n.d.	n.d.	1	n.d.	0.93	0.6	n.d.	n.d.	n.d.	n.d.	n.d.	n.d.	n.d.	n.d.
Yb	n.d.	0.93	n.d.	n.d.	n.d.	n.d.	n.d.	n.d.	2.69	n.d.	2.39	1.6	n.d.	n.d.	n.d.	n.d.	n.d.	n.d.	n.d.	n.d.
Lu	n.d.	0.13	n.d.	n.d.	n.d.	n.d.	n.d.	n.d.	0.38	n.d.	0.42	0.25	n.d.	n.d.	n.d.	n.d.	n.d.	n.d.	n.d.	n.d.

	Sausfjellet pluton								Contact granites							Granitic rocks of the Bindal batholith				
sample	VF55	73.14	VF54	73.20	73.28	91.39	73.05	91.26	72.52	VF57	N17 91	N19 91	VF58	VF47	N21 91	N87-42	N87-43	VF60	VF61	VF40
SiO_2	49.54	50.05	51.64	53.34	53.79	54.25	55.54	59.32	64.40	64.43	64.43	64.86	66.76	67.60	68.64	69.73	70.99	71.19	71.95	71.95
TiO_2	0.82	0.83	0.52	0.69	0.67	1.09	1.09	1.06	0.72	0.86	0.91	0.84	0.55	0.53	0.50	0.26	0.26	0.27	0.25	0.21
Al_2O_3	13.21	17.14	16.24	16.93	17.91	17.21	17.43	17.41	16.72	16.22	16.36	16.75	16.00	16.06	16.22	16.01	15.43	14.71	14.95	15.40
Fe_2O_3	10.96	9.39	7.06	8.29	8.21	9.49	8.89	6.54	5.48	5.45	6.10	5.73	3.94	3.54	3.19	2.05	1.46	2.38	1.49	1.64
MnO	0.18	0.17	0.15	0.15	0.15	0.15	0.14	0.10	0.09	0.11	0.09	0.06	0.08	0.03	0.03	0.03	0.02	0.05	0.03	0.05
MgO	13.65	7.91	8.06	6.99	5.06	4.80	3.37	2.50	0.94	1.37	1.29	1.39	0.76	0.61	0.58	0.69	0.65	0.31	0.50	0.50
CaO	8.84	11.12	13.07	8.93	8.35	7.97	6.68	4.92	2.69	1.84	2.55	1.87	2.36	2.35	2.03	1.63	1.79	1.13	1.49	2.10
Na_2O	1.44	2.56	2.35	3.42	3.88	3.56	3.63	3.74	3.03	2.89	3.07	2.29	3.58	3.44	3.00	3.91	3.81	3.54	3.70	5.45
K_2O	1.16	0.78	0.45	0.66	1.26	1.74	2.31	3.78	4.48	5.91	4.50	5.34	5.15	5.30	4.96	4.97	4.55	5.98	4.84	2.03
P_2O_5	0.02	0.03	0.03	0.26	0.23	0.27	0.30	0.41	0.31	0.14	0.18	0.13	0.22	0.19	0.24	0.10	0.10	0.09	0.15	0.08
LOI	0.56	n.d.	0.61	n.d.	n.d.	0.03	n.d.	0.37	n.d.	0.61	0.32	0.58	0.58	0.37	0.78	0.63	1.13	0.40	0.75	0.32
Total	100.38	99.98	100.18	99.66	99.51	100.56	99.38	100.15	98.86	99.83	99.80	99.84	99.98	100.02	100.17	100.01	100.19	100.05	100.10	99.73
Rb	40	16	7	15	40	37	88	114	173	189	135	165	156	154	229	239	222	210	244	127
Sr	276	439	481	556	586	545	598	520	201	179	242	172	198	212	202	171	223	96	143	328
Zr	61	68	56	47	74	120	215	356	478	486	388	510	347	311	332	123	130	220	129	113
Y	27	47	24	24	25	25	36	40	81	62	49	76	43	37	31	22	21	21	18	14
Nb	5	n.d.	2	n.d.	n.d.	13	14	20	n.d.	24	26	27	40	22	28	15	13	19	12	10
Ba	353	173	182	319	417	612	664	843	1200	885	1052	895	925	971	886	302	328	400	346	231
Sc	25	39.6	33	27.2	24.1	n.d.	18.8	n.d.	9.7	12	n.d.	n.d.	8	6	n.d.	6	2	5	6	2
V	175	159	130	135	170	306	161	108	32	47	55	33	30	31	13	18	16	5	16	17
Cr	211	298	236	72	60	46	54	31	60	28	34	54	10	7	12	15	22	4	5	12
Ni	184	51	49	27	17	27	40	24	2	17	11	17	4	6	4	8	4	3	3	0
Cu	26	22	21	15	4	15	18	19	6	28	18	12	10	7	3	<1	<1	5	4	1
Zn	66	69	50	70	77	80	85	73	79	56	70	78	54	53	62	35	28	41	30	30
Th	5	n.d.	2	n.d.	n.d.	n.d.	n.d.	n.d.	n.d.	49	n.d.	n.d.	24	29	n.d.	18	19	30	12	11
La	11	n.d.	20	24.6	n.d.	n.d.	50.7	n.d.	n.d.	70	n.d.	n.d.	50	127	n.d.	36	28	72	24	9
Ce	14	n.d.	31	48	n.d.	n.d.	100	n.d.	n.d.	151	n.d.	n.d.	106	67	n.d.	44	48	150	46	22
Nd	20	n.d.	21	22	n.d.	n.d.	42	n.d.	n.d.	61	n.d.	n.d.	40	57	n.d.	19	24	45	22	17
Sm	n.d.	n.d.	n.d.	4.26	n.d.	n.d.	7.86	n.d.	n.d.	n.d.	n.d.	n.d.	n.d.	n.d.	n.d.	n.d.	n.d.	n.d.	n.d.	n.d.
Eu	n.d.	n.d.	n.d.	1.42	n.d.	n.d.	2	n.d.	n.d.	n.d.	n.d.	n.d.	n.d.	n.d.	n.d.	n.d.	n.d.	n.d.	n.d.	n.d.
Tb	n.d.	n.d.	n.d.	0.6	n.d.	n.d.	0.9	n.d.	n.d.	n.d.	n.d.	n.d.	n.d.	n.d.	n.d.	n.d.	n.d.	n.d.	n.d.	n.d.
Yb	n.d.	n.d.	n.d.	2.12	n.d.	n.d.	3.45	n.d.	n.d.	n.d.	n.d.	n.d.	n.d.	n.d.	n.d.	n.d.	n.d.	n.d.	n.d.	n.d.
Lu	n.d.	n.d.	n.d.	0.32	n.d.	n.d.	0.52	n.d.	n.d.	n.d.	n.d.	n.d.	n.d.	n.d.	n.d.	n.d.	n.d.	n.d.	n.d.	n.d.

* Major element concentrations in weight percent, trace elements in ppm. n.d., not determined

\+ 72.73 & VF42 from low SiO_2 group, VF43, 91.12, & 72.80 from high K_2O group VF41, 72.84, & VF44 from high SiO_2 group

The second stage can be divided into three groups on the basis of SiO_2 and K_2O abundances (Fig. 5). Monzonitic samples from the western side of the pluton have the lowest SiO_2 contents; whereas quartz monzonitic rocks on the eastern side have high SiO_2 contents. Monzonitic samples from the area between these two groups have the highest K_2O values (at constant SiO_2) in the pluton. Sr behaves as a compatible element in the second stage, whereas Rb and Zr are incompatible. The REE abundances of second-stage

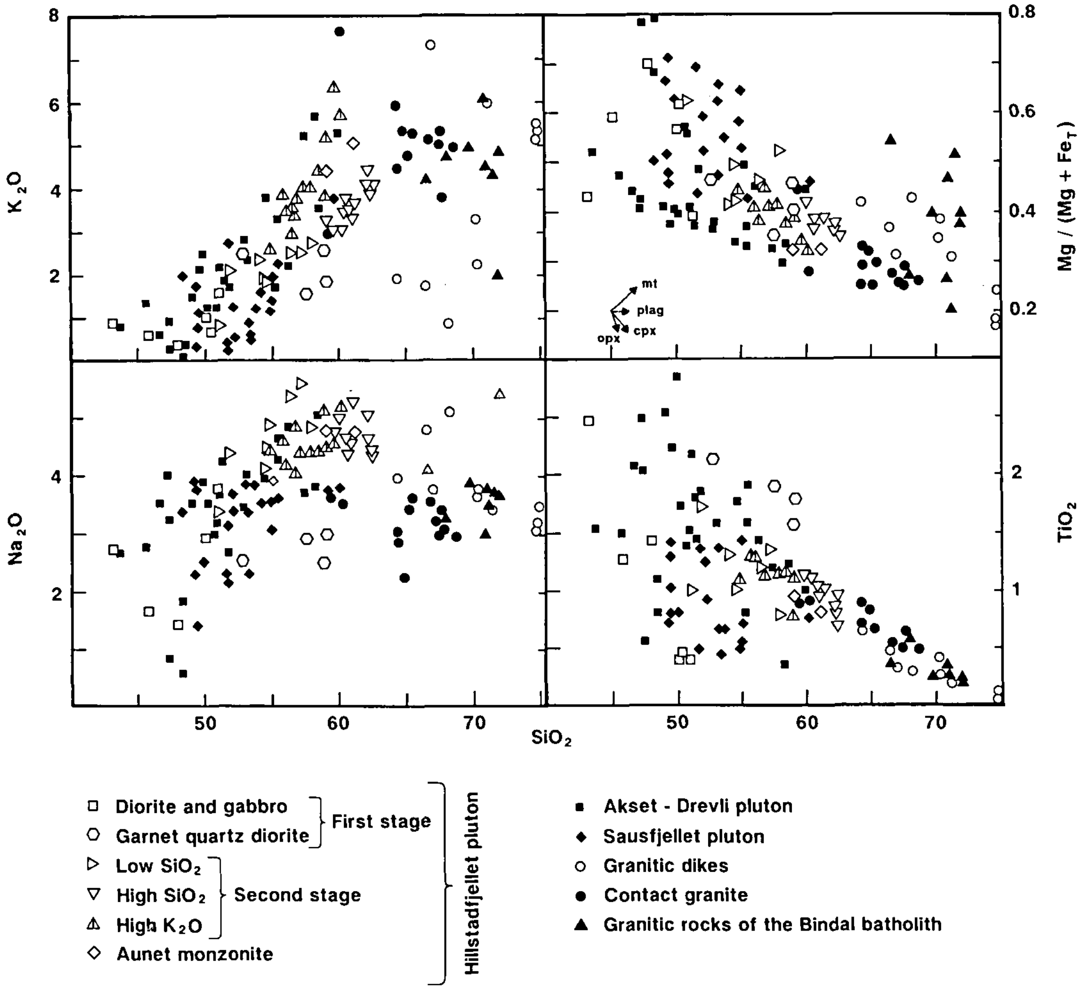

Fig. 5. Variation of (A) K_2O, (B) Na_2O, (C) Mg/(Mg+Fe_T), and (D) TiO_2 plotted as a function of SiO_2 content. Fe_T = total Fe. In C, arrows schematically show the effects of fractionation of magnetite (mt), plagioclase (plag), augitic clinopyroxene (cpx), and orthopyroxene (opx) from a parental magma.

samples increase with increasing SiO_2 and the $(Ce/Yb)_N$ ratio is virtually constant ($\approx$14). Although negative Eu anomalies are apparent, they are slight (Fig. 7a). The most evolved samples from the second stage of this pluton are compositionally similar to the Aunet monzonite although one sample of the Aunet monzonite has a much larger negative Eu anomaly (not shown in Fig. 7).

The Akset-Drevli pluton is also alkali-calcic (alkali-lime index about 53). The analyses show considerable scatter in Al_2O_3, CaO, and Na_2O, as might be expected in such plagioclase-phyric rocks. In general, the pluton has lower Mg/(Mg+Fe_T) ratios and higher (but widely scattered) TiO_2 contents than the Hillstadfjellet and Sausfjellet plutons (Fig. 5). REE abundances and patterns are similar to the Hillstadfellet pluton but $(Ce/Yb)_N$ values are slightly higher (19), with the exception of two dikes. One dike is a late-stage gabbro which has lower total REE and lower $(Ce/Yb)_N$ (=7.5) than the rest of the pluton (Fig. 7b); the pattern also shows a downward concavity among the light REE. The other dike is a monzodiorite with plagioclase phenocrysts and K-feldspar xenocrysts (?) that intrudes a marble screen near the northern contact of the pluton. It is

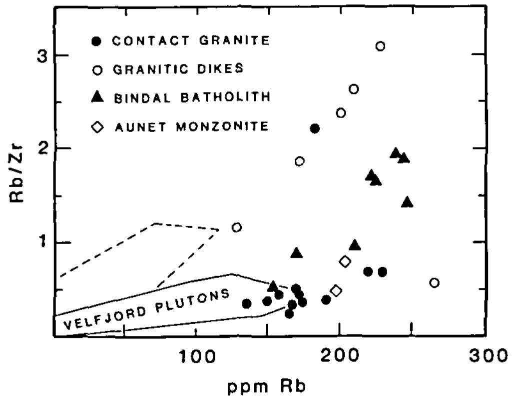

Fig. 6. Rb/Zr (weight ratio) versus Rb. The field enclosed by a solid line represents over 90% of samples from the Velfjord plutons; the field enclosed by a dashed line encloses Rb-rich samples, predominantly from the Hillstadfjellet pluton.

characterized by its high total REE, pronounced negative Eu anomaly, and lower $(Ce/Yb)_N$ ratio (=11; Fig. 7b).

The Sausfjellet pluton is distinct from the other Velfjord plutons in its lower TiO_2 contents (Fig. 5) and higher alkali-lime index (=56, calc-alkalic). Al_2O_3, Na_2O, CaO, and TiO_2 show a great deal of scatter. Sr behaves as an incompatible element in the Sausfjellet pluton unlike the second stage of the Hillstadfjellet pluton. The REE abundances of this pluton display a relatively large range considering the small range of SiO_2 values. The normalized patterns of three samples (73.65, 91.20, 91.22A) have relatively steep slopes ($(Ce/Yb)_N$ = 14-18). All three were collected near contacts and all are quartz-bearing; sample 73.65 is a late-stage quartz diorite. The remaining samples are dioritic and have patterns with shallower slopes ($(Ce/Yb)_N$ from 3 to 7). Among these samples, the increase in $(Ce/Yb)_N$ is accompanied by an increase in total REE abundances (Fig. 7c).

The granitic rocks of the Bindal Batholith, granites collected near the margins of the Velfjord plutons (contact granites), and granitic dikes in the plutons are generally calc-alkalic and all but one are peraluminous. Six of the contact granites have Al/(Ca+Na+K) greater than 1.1 (i.e., strongly peraluminous) as do four granitic dikes that cut the plutons. None of the granitic rocks of the Bindal Batholith are strongly peraluminous. The higher SiO_2, Rb, and $Mg/(Mg+Fe_T)$ and generally lower Zr, Sr, and TiO_2 of the granitic rocks of the Bindal Batholith serve to distinguish them from the contact granites (Table 1; Figs. 5 and 6). In addition, the Rb/Zr ratio of the various types of granitic rocks in the area serve to distinguish them from one another (Fig. 6). The contact granites have a low, nearly constant ratio, whereas the Rb/Zr ratios of the granitic dikes and the granites of the Bindal Batholith increase with increasing Rb content and are distinct from each other (Fig. 6).

REE abundances in the contact granites display a wide range of concentrations (Fig. 7d), with the highest abundances of the heavy REE, the lowest $(Ce/Yb)_N$ ratios ($\approx$12), and the only negative Eu anomalies in the garnet-bearing granites. A garnet-free, two-mica-bearing granitic dike in the Sausfjellet pluton has the highest REE slope ($(Ce/Yb)_N$=40), which is largely due to the low concentrations of the heavy REE.

Discussion

The close spatial relationship between the Velfjord plutons and the contact granites suggests that the granites resulted from local anatexis caused by heat from the adjacent dioritic magmas. The volume of the contact granites and the gradation from granite to migmatite with distance from the dioritic plutons suggests that the host pelitic rocks were partially molten at the time of emplacement of the dioritic magmas. If this interpretation is correct, the Velfjord plutons must have been emplaced during or just after the peak of regional metamorphism in the region, which is consistent with Kollung's (1967) view that the plutons were syntectonic. Accumulation of granitic melts near the dioritic plutons may have been enhanced by disruption of the host migmatites during intrusion and by contraction of the dioritic magmas during cooling and crystallization.

Petrographic evidence suggests that deformation of the dioritic rocks, granitic dikes, and contact granites began when melt was present and continued, at least locally, through cooling to greenschist facies conditions. The contact granites show the greatest degree of strain because of this continuum of deformation from synmagmatic to submagmatic conditions and because they have low solidus temperatures and abundant, easily-deformed quartz.

Asymmetric zoning patterns similar to those

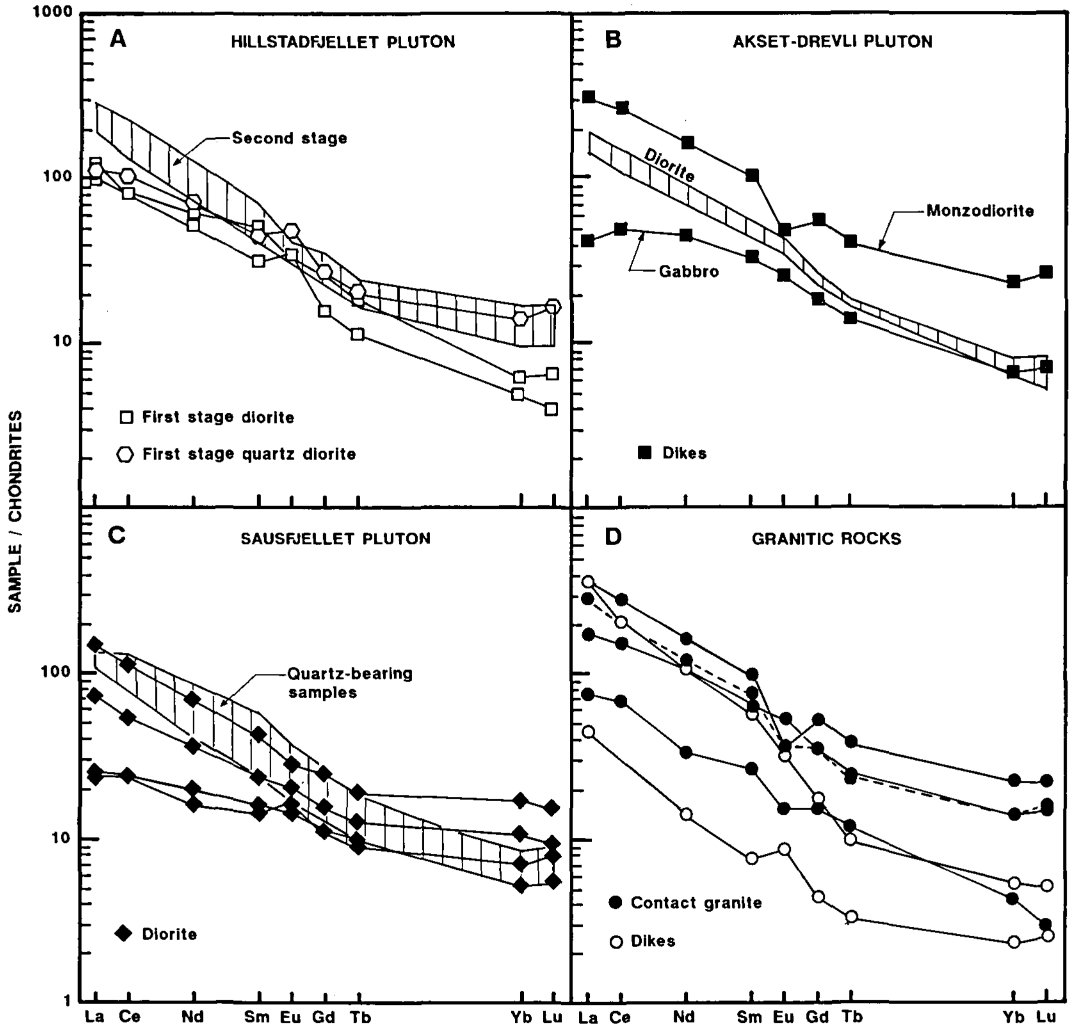

Fig. 7. Chondrite-normalized (Haskin et al. 1968) REE patterns. A. Hillstadfellet pluton. The lined field encloses the patterns of second stage samples. B. Akset-Drevli pluton. The lined field encloses patterns of dioritic samples from the pluton. C. Sausfjellet pluton. Individual patterns are for quartz-poor or quartz-free samples, lined area encloses patterns of quartz-bearing samples. D. Granitic rocks.

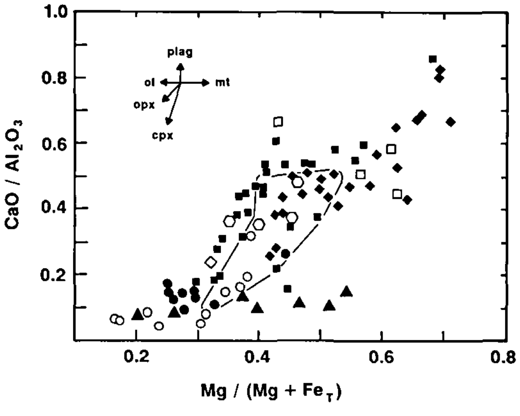

Fig. 8. Weight ratio of CaO/Al$_2$O$_3$ plotted against Mg/(Mg+Fe$_T$). The field encloses data from the second stage of the Hillstadfjellet pluton. All other symbols as in Fig. 5. The arrows indicate the effects of fractionation of olivine (ol), orthopyroxene (opx), augitic clinopyroxene (cpx), magnetite (mt), and plagioclase (plag).

observed in the Hillstadfjellet and Sausfjellet plutons have been reported elsewhere (e.g., Bateman et al. 1963, Flood & Shaw 1979, Barnes et al. 1986). Such asymmetry has been ascribed either to tilting and erosion of a vertically-zoned pluton (Flood & Shaw 1979, Barnes et al. 1986) or to non-coaxial filling of an expanding pluton (Hutton 1988a). In the latter case, the plutons have generally been shown to have intruded in dilatant zones in a shear couple (Hutton, 1988a&b). Similar models were developed for the emplacement of gabbro and granodiorite in the Sunnhordland Batholith in western Norway (Andersen et al. 1991). We suggest that the asymmetric zoning patterns of the Hillstadfellet and Sausfjellet plutons may have resulted from intrusion into a dilatant zone of a sinistral shear couple. This idea is consistent with the position of the Velfjord plutons in a weakly-lineated NNW-SSE-trending zone (the dilatant zone) between two strongly lineated NE-SW-trending zones. In such an instance, elongate intrusions such as the Akset-Drevli pluton and stage 1 of the Hillstadfjellet pluton would have a NNW-SSE orientation, parallel to that of the dilatant zone. This idea is consistent with asymmetric zoning in the Hillstadfjellet and Sausfjellet plutons, with syntectonic emplacement of the Velfjord plutons soon after peak metamorphism, D_2 deformation, and thrusting within the HNC, and can explain the peridotite xenoliths in the Akset-Drevli pluton as having originated in the middle thrust sheet. It also permits in situ formation of the contact granites in a ductile, high-temperature environment. The high-temperature, syn- and post-emplacement deformation of the plutons and contact granites can thus be explained by deformation during the waning stages of D_2 tectonism.

The petrogenesis of the plutons and related granitic rocks can only be determined with detailed elemental and isotopic modelling (in progress). However, on the basis of currently available data, we can make several deductions about the petrology of the Velfjord plutons. (1) The presence of olivine in the Akset-Drevli pluton indicates that at least some of the parental magmas had an ultramafic source and originated in the lower crust or upper mantle. However, the general lack of olivine and the intermediate to low $Mg/(Mg+Fe_T)$ values in nearly all samples of the Akset-Drevli pluton indicate that the parental magmas had undergone differentiation prior to emplacement. (2) The fact that the plutons are distinctly different in terms of $Mg/(Mg+Fe_T)$ and TiO_2 (in particular) suggests that the parental magmas were compositionally distinct. These distinctions could have arisen from different primary magma compositions; but may also indicate differences in evolutionary paths. For example, the relatively Fe-rich nature of the Akset-Drevli pluton implies magmatic evolution at low $f(O_2)$. In contrast, the low TiO_2 in the Sausfjellet pluton could have resulted from an initially TiO_2-poor parental magma or from early removal of Fe-Ti oxides at relatively high $f(O_2)$, both of which are consistent with the calc-alkalic nature of the pluton. (3) The conspicuous scatter among the major-element and compatible trace-element compositions of the Sausfjellet and Akset-Drevli plutons and the first stage of the Hillstadfjellet pluton can be explained in terms of accumulation and/or removal of variable amounts of plagioclase, pyroxene (especially clinopyroxene), and oxide phases. In Figs. 5c and 8, the effects of fractionation of these phases are schematically shown. The compositions of most samples from the Sausfjellet pluton can be explained by clinopyroxene + plagioclase accumulation and the scatter shown by the Akset-Drevli pluton can be explained as the result of cpx ± plagioclase ± magnetite accumulation. Schlieren banding, which is common in the Sausfjellet pluton, is generally thought to form as the result of crystal segregation during magmatic flow. This mechanism can probably explain much of the wide compositional scatter among rocks in the pluton. (4) The alkali-rich compositions of the two northern plutons and the differences in composition and intensive variables among and within plutons may have been caused by assimilation of crustal rocks or mixing with crustal melts. For example, the three distinct compositional groups of the second stage of the Hillstadfjellet pluton probably do not represent the products of simple fractional crystallization or accumulation from a single parent. The plot of K_2O against SiO_2 (Fig. 5A) is suggestive that the SiO_2-rich group could be the result of mixing of monzonitic and granitic melts such as the contact granites.

The compositional distinctions between the contact granites, granites typical of the Bindal Batholith, and granitic dikes in the dioritic plutons implies distinct origins for the three groups. It also indicates that the dikes in the plutons are probably not offshoots of nearby Bindal granites, as suggested by Kollung (1967), or of the contact granites. Therefore, the fact that granitic dikes cut the Velfjord plutons should not be taken as evidence for the relative timing between Bindal granites and Velfjord diorites.

The contact granites display mineral assemblages and chemical compositions typical of derivation by partial melting of pelitic source rocks (White & Chappell, 1977), which is consistent with the idea that the contact granites resulted from nearly complete in-situ anatexis of host rocks that were partly molten at the time of intrusion. The positive correlation between Rb/Zr and Rb in the granitic dikes (Fig. 6) is primarily a function of decreasing Zr content with increasing Rb. If these dikes are differentiates of the dioritic magmas, this relationship may indicate that zircon was a late fractionating phase; however, it is also compatible with an origin by partial melting with zircon residual in the source.

A similar relationship between Rb/Zr and Rb among the granitic rocks of the Bindal Batholith suggests similar conclusions may be reached. In general however, the chemical and isotopic compositions of granites of the Bindal Batholith are not suggestive of derivation from pelitic source rocks typical of the Uppermost Allochthon (Table 1; Ø. Nordgulen, unpublished data), but indicate an origin by processes that operated deeper in the crust. However, our sampling of these rocks in the Velfjord area is too sparse to justify further speculation.

Conclusions

The Velfjord plutons represent intrusion of mafic and intermediate magmas into the HNC during the metamorphic peak or soon thereafter. At least two of the plutons had more than one parental magma and each parental magma followed different evolutionary paths. Much of the compositional variation in the Akset-Drevli and Sausfjellet plutons can be ascribed to variable accumulation of cpx, plagioclase, and oxide minerals. Each pluton caused in-situ anatexis of pelitic migmatites in the host rocks, which resulted in lenses of peraluminous granite adjacent to the dioritic bodies. Mixing of these contact granitic melts with magma of the plutons may have caused some of the compositional variations observed. The deformation of the plutons and the contact granites and the zoning patterns of the northern and southern plutons suggest that deformation accompanied intrusion in a dilatant zone of a regional sinistral shear couple. This interpretation has significant implications not only for the origin and evolution of the Velfjord plutons but for the entire Bindal Batholith, and deserves detailed structural, geochronological, and isotopic investigation. Finally, the compositional complexities among the Velfjord plutons as well as the variety of granitic rocks in the area emphasize the need to consider multistage evolutionary paths in the development of the Bindal Batholith.

Acknowledgements

This research was completed while C. Barnes was at the *Norwegian Institute of Technology in Trondheim under the* auspices of the Fulbright-Hays Program for International Exchange of Scholars. Prestvik's fieldwork in 1972 and 1973 was supported by Nansenfondet; field and analytical work in 1990 and 1991 were supported by NAVF grants 440.90/002, 440.91/004 and 441.91/011 to Prestvik. Ø. Nordgulen wishes to acknowledge financial support from the Geological Survey of Norway and from NTNF grant MT 0020.20343. Finally, we wish to thank I. Vokes and I. Rømme for the assistance with XRF analyses.

References

Andersen,T.B., Nielsen,P., Rykkelid,E., & Sølna,H. 1991. Melt-enhanced deformation during emplacement of gabbro and granodiorite in the Sunnhordland Batholith, west Norway. *Geol. Mag. 128,* 207-226.

Barnes, C.G., Rice, J.M. & Gribble, R.F. 1986: Tilted plutons in the Klamath Mountains of California and Oregon. *J. geophys. Res. 91,* 6059-6071.

Bateman, P.C., Clark, L.D., Huber, N.K., Moore, J.G. & Rinehart, C.D. 1963: The Sierra Nevada Batholith--A synthesis of recent work across the central part. *U.S. Geol. Surv. Prof Paper 414-D,* 46 pp.

Bucher-Nurminen, K. 1988: Metamorphism of ultramafic rocks in the Central Scandinavian Caledonides. *Nor. geol. unders. Special Publ. 3,* 86-95.

Flood, R.H. & Shaw, S.E. 1979: K-rich cumulate diorite at the base of a tilted granodiorite pluton from the New England batholith, Australia. *J. Geol. 87,* 417-425.

Haskin, L.A., Haskin, M.A., Frey, F.A. & Wildeman, T.R. 1968: Relative and absolute terrestrial abundances of the rare earths. *In:* Ahrens, L.H., ed. *Origin and distribution of the elements,* Pergamon, Oxford, England, 889-912.

Hutton, D.H.W. 1988a: Igneous emplacement in a shear-zone termination: The biotite granite at Strontian, Scotland. *Geol. Soc. Amer. Bull. 100,* 1392-1399.

Hutton, D.H.W. 1988b: Granite emplacement mechanisms and tectonic controls: inferences from deformation studies. *Trans. Royal Soc. Edinburgh: Earth Sciences 79,* 245-255.

Kollung, S. 1967: Geologiske undersøkelser i det sørlige Helgeland og nordlige Namdal. *Nor. geol. unders. 254,* 95 pp.

Myrland, R. 1972: Velfjord. Beskrivelse til det berggrunnsgeologiske gradteigskart I 18 - 1:100 000. *Nor. geol. unders. 274,* 30 pp.

Prestvik, T. 1974: Norwegian chromian ugrandite-garnets. *Nor. Geol. Tidsskr. 54,* 177-182

Stephens, M.B., Furnes, H., Robins, B. & Sturt, B.A. 1985: Igneous activity within the Scandinavian Caledonides. *In:* Gee, D.G. & Sturt, B.A. (eds.), *The Caledonide Orogen - Scandinavia and related areas.* John Wiley and Sons Ltd., Chichester, 623-656.

Thorsnes, T. & Løseth, H. 1991: Tectonostratigraphy in the Velfjord-Tosen region, southwestern part of the Helgeland Nappe Complex, Central Norwegian Caledonides. *Nor. geol. unders. Bull. 421,* 1-18.

Tørudbakken, B.O. & Mickelson, M. 1986: A Rb/Sr study from the Mosjøen unit, Helgeland Nappe Complex and its bearing on the timing of tectono-metamorphic events within the Uppermost Allochthon, Central Scandinavian Caledonides, Norway. *Nor. Geol. Tidsskr. 66,* 263-270.

White, A.J.R. & Chappell, B.W. 1977: Ultrametamorphism and granitoid genesis. *Tectonophysics 43,* 7-22.

Manuscript received March 1992; revised typescript June 1992; accepted June 1992.